

Dispersive determination of the fourth generation lepton masses

Hsiang-nan Li*

Institute of Physics, Academia Sinica, Taipei, Taiwan 115, Republic of China

(Dated: December 20, 2024)

We continue our previous determination of the masses of the sequential fourth generation quarks in an extension of the Standard Model, and predict the mass m_4 (m_L) of the fourth generation neutrino ν_4 (charged lepton L) by solving the dispersion relations associated with heavy fermion decays. The results $m_4 \approx 170$ GeV and $m_L \approx 270$ GeV are extracted from the dispersive analyses of the $t \rightarrow de^+\nu_4$ and $L^- \rightarrow \nu_1 \bar{t}d$ decay widths, respectively, where t (d , e^+ , ν_1) denotes a top quark (down quark, positron, light neutrino). The predictions are cross-checked by examining the $L^- \rightarrow \nu_4 \bar{u}d$ decay, \bar{u} being an anti-up quark. It is shown that the fourth generation leptons with the above masses survive the current experimental bounds from Higgs boson decays into photon pairs and from the oblique parameters. We also revisit how the existence of the fourth generation leptons impacts the dispersive constraints on the neutrino masses and the Pontecorvo–Maki–Nakagawa–Sakata (PMNS) matrix elements. It is found that the unitarity of the 3×3 PMNS matrix holds well up to corrections of $O(m_\nu^2/m_W^2)$, m_ν (m_W) being a light neutrino (the W boson) mass, whose mixing angles and CP phase prefer the values $\theta_{12} \approx 34^\circ$, $\theta_{23} \approx 47^\circ$, $\theta_{13} \approx 5^\circ$ and $\delta \approx 200^\circ$ in the normal-ordering scenario for neutrino masses.

I. INTRODUCTION

We have performed dispersive analyses on the flavor structure of the Standard Model (SM) in a series of publications recently [1–4]. Sufficient clues for understanding the mass hierarchy and the distinct mixing patterns of quarks and leptons have been accumulated, which suggest that the scalar sector could be stringently constrained by the internal consistency of SM dynamics. We were then motivated to explore the sequential fourth generation model as a natural and simple extension of the SM, for which no additional free parameters need to be introduced. The masses of the fourth generation quarks b' and t' were determined by studying neutral quark state mixing through box diagrams, i.e., the $Q\bar{q}-\bar{Q}q$ mixing with Q (q) being a heavy (light) quark [5]. The idea is to treat the dispersion relation obeyed by a mixing observable as an inverse problem with the input from the perturbative evaluation of the box diagrams [6–8]. It was demonstrated that a solution to the dispersion relation demands a specific mass of the heavy quark [5]; the common mass $m_{b'} \approx 2.7$ TeV ($m_{t'} \approx 200$ TeV) was obtained from the dispersive analyses of the box diagrams involving the intermediate quark channels ut and ct (db' , sb' and bb').

For an extension of the SM to be anomaly free, the existence of the fourth generation quarks requires that of the fourth generation leptons. The intensive practice of our formalism guarantees that the masses of the fourth generation leptons can also be predicted by investigating appropriate observables, such as heavy fermion decays. The Z boson decay data [9] have indicated that the fourth generation neutrino ν_4 and charged lepton L are heavier than half of the Z boson mass. Hence, we examine the dispersion relation for the semileptonic top quark decay $t \rightarrow de^+\nu_4$ in the framework similar to the one in [1], d (e^+) being a down quark (positron), and show that the reproduction of the top quark mass $m_t \approx 173$ GeV leads to the ν_4 mass $m_4 \approx 170$ GeV. The study of the hadronic decay $L^- \rightarrow \nu_i \bar{t}d$, where ν_i , $i = 1, 2$ or 3 , represents a light neutrino, yields the L mass $m_L \approx 270$ GeV, as $m_t \approx 173$ GeV is input into the corresponding dispersion relation. We then substantiate the above heavy lepton masses by checking the dispersion relation for the hadronic decay $L^- \rightarrow \nu_4 \bar{u}d$ with an anti-up quark \bar{u} . A positron, light neutrinos, and light quarks in final states are all treated as massless particles [1] for simplicity. The simultaneous satisfaction of the dispersion relations for the three different processes by our predictions should not be a coincidence.

The merits of the sequential fourth-generation model have been summarized in [5]; it provides a dynamical mechanism for electroweak symmetry breaking by means of heavy fermion condensates [10, 11], realizes electroweak baryogenesis through the first-order phase transition [12], and offers a viable source of CP violation for the baryon asymmetry of the Universe [13]. It was pointed out that the fourth generation quarks b' and t' with the masses above a TeV scale form bound states in a Yukawa potential [14, 15]. The contributions from the $\bar{b}'b'$ scalars to the Higgs boson production via gluon fusion and to the Higgs decay into a photon pair, $H \rightarrow \gamma\gamma$, were estimated to be of $O(10^{-3})$ and $O(10^{-2})$ of the top quark one [5], respectively. These estimates illustrated why these superheavy quarks bypass the experimental constraints from Higgs boson production and decay [16]. The fourth generation leptons, with the masses of the electroweak scale, are too light to form bound states. We thus calculate the contribution from the

* Corresponding author, E-mail: hnli@phys.sinica.edu.tw

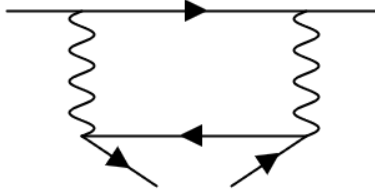


FIG. 1: Box diagram for a heavy fermion decay, where the wavy lines represent W bosons.

charged lepton of the mass 270 GeV to the $H \rightarrow \gamma\gamma$ decay width $\Gamma_{\gamma\gamma}$, and evince that its effect is within the current uncertainties of $\Gamma_{\gamma\gamma}$ measurements. The impact on the oblique parameters from the fourth generation quarks and leptons, inspected based on the formulas supplied in [17], is also allowed by the experimental errors of the oblique parameters. The search for heavy neutral leptons at colliders within the mass range from GeV to the electroweak scale has been updated in [18].

At last, we revisit how the existence of the fourth generation leptons modifies the constraints on the neutrino masses and the Pontecorvo–Maki–Nakagawa–Sakata (PMNS) matrix elements. These constraints were derived for the case with three generations of neutrinos in [3], which favor the neutrino masses in the normal ordering (NO), instead of the inverted ordering (IO), in view of the consistency with the observed PMNS matrix elements [19, 20]. We repeat the analysis with four generations of neutrinos here, and find that the unitarity of the 3×3 PMNS matrix holds quite well. Namely, the fourth generation leptons barely mix with the three light generations. The theoretical preference on the NO scenario is confirmed, and the aforementioned constraints are better respected. Explicitly speaking, the known mass squared differences among the neutrinos are linked to the mixing angles $\theta_{12} \approx 34^\circ$, $\theta_{23} \approx 47^\circ$ and $\theta_{13} \approx 5^\circ$, and the CP phase $\delta \approx 200^\circ$, close to the measured values for the NO scenario. In this sense, the data for the PMNS mixing angles have revealed the possible existence of the fourth generation leptons. As the same formalism is applied to the quark mixing, the unitarity of the 3×3 Cabibbo-Kobayashi-Maskawa matrix is expected to be violated at the level of $m_b^2/m_W^2 \sim 10^{-3}$, m_b (m_W) being the b quark (W boson) mass.

The rest of the paper is organized as follows. We briefly recollect the construction of a dispersion relation based on analyticity of a physical observable and its solution in Sec. II. The masses of the fourth generation leptons are extracted from the dispersion relations for the $t \rightarrow de^+\nu_4$ and $L^- \rightarrow \nu_1\bar{t}d$ decays, and cross-checked by means of the $L^- \rightarrow \nu_4\bar{u}d$ decay in Sec. III. The experimental bounds from Higgs boson decays into photon pairs and from the oblique parameters on the sequential fourth generation model are scrutinized in Sec. IV. We discuss the dispersive constraints on the neutrino masses and the PMNS matrix elements in the presence of the fourth generation leptons in Sec. V. The mixing angles and the CP phase involved in the 3×3 PMNS matrix are solved for and confronted with the data. Section VI contains the conclusion; our observations encourage the search for the fourth generation leptons at the (high-luminosity) large hadron collider or a muon collider.

II. DISPERSION RELATION AND ITS SOLUTION

Consider the analytical amplitude $\Pi(m_Q^2)$ associated with the box diagram in Fig. 1, whose imaginary part gives the inclusive decay width $\Gamma(m_Q)$ of a heavy fermion Q of the mass m_Q . The diagram describes the semileptonic decay $t \rightarrow dW^+ \rightarrow de^+\nu_4$ or the hadronic decay $L^- \rightarrow \nu_1W^- \rightarrow \nu_1\bar{t}d$ to be explored in the next section. Here the first generation neutrino ν_1 is representative and can be replaced by ν_2 or ν_3 . Because a top quark is heavier than a W boson, the latter cannot be integrated out to get the effective weak Hamiltonian for the above decays. The operator definition of the amplitude $\Pi(m_Q^2)$ is thus lengthier than in Ref. [1], where decays of lighter fermions were studied. For example, the amplitude related to the semileptonic decay $t \rightarrow de^+\nu_4$ is written as

$$\Pi(m_t^2) \propto \frac{1}{2m_t} \int d^4x H^{\mu\nu}(x) \langle t | J_\mu^\dagger(x) J_\nu(0) | t \rangle, \quad (1)$$

in which the function

$$H^{\mu\nu}(x) = \int \frac{d^4k_1}{(2\pi)^4} \frac{d^4k_2}{(2\pi)^4} \exp[-ix \cdot (k_1 + k_2)] \frac{k_1^\mu k_2^\nu + k_1^\nu k_2^\mu - g^{\mu\nu} k_1 \cdot k_2}{k_1^2 (k_2^2 - m_4^2) [(k_1 + k_2)^2 - m_W^2]^2}, \quad (2)$$

collects the contribution from the leptonic part, and $J_\mu = \bar{d}\gamma_\mu P_L t$ with the projector $P_L = (1 - \gamma_5)/2$ is the $V - A$ current. The overall coefficient, irrelevant to the discussion, has been omitted. The construction of Eq. (1) follows the one for the Drell-Yan cross section in [21].

We have the identity from the contour integration for $\Pi(m_Q^2)$ [7],

$$\frac{1}{2\pi i} \oint \frac{\Pi(m^2)}{m^2 - m_Q^2} dm^2 = 0, \quad (3)$$

whose contour consists of two pieces of horizontal paths above and below the branch cut along the positive real axis, a small circle around the pole $m^2 = m_Q^2$ located on the positive real axis and a circle C_R of the large radius R . The above integral vanishes, for the contour encloses unphysical regions without poles. Equation (3) is rewritten as

$$\text{Re}\Pi(m_Q^2) = \frac{1}{\pi} \int_{m_F^2}^{R^2} \frac{\text{Im}\Pi(m^2)}{m^2 - m_Q^2} dm^2 + \frac{1}{2\pi i} \int_{C_R} \frac{\Pi(m^2)}{m^2 - m_Q^2} dm^2, \quad (4)$$

where the hadronic threshold m_F sums the masses in the lightest final state. The contribution along the small clockwise circle gives the real part $\text{Re}\Pi(m_Q^2)$ on the left-hand side. The contribution from the horizontal paths along the positive real axis leads to the dispersive integral of the imaginary part $\text{Im}\Pi(m^2)$. It contains nonperturbative dynamics associated with light hadronic final states near the threshold, where the decay becomes exclusive. The integrand $\Pi(m^2)$, taking values along the large counterclockwise circle C_R , has been reliably approximated by $\Pi^P(m^2)$ from the perturbative evaluation of Fig. 1. The perturbative result $\Pi^P(m_Q^2)$ from Fig. 1 certainly obeys a similar dispersion relation because of the analyticity,

$$\text{Re}\Pi^P(m_Q^2) = \frac{1}{\pi} \int_{m_f^2}^{R^2} \frac{\text{Im}\Pi^P(m^2)}{m^2 - m_Q^2} dm^2 + \frac{1}{2\pi i} \int_{C_R} \frac{\Pi^P(m^2)}{m^2 - m_Q^2} dm^2, \quad (5)$$

with the quark-level threshold m_f in the dispersive integral, above which the imaginary part $\text{Im}\Pi^P(m^2)$ is defined.

We equate $\text{Re}\Pi(m_Q^2)$ and $\text{Re}\Pi^P(m_Q^2)$, i.e., Eqs. (4) and (5) at large enough $m_Q \gg m_F$, where a perturbation theory is trustworthy, arriving at

$$\int_{m_F^2}^{R^2} \frac{\text{Im}\Pi(m^2)}{m^2 - m_Q^2} dm^2 = \int_{m_f^2}^{R^2} \frac{\text{Im}\Pi^P(m^2)}{m^2 - m_Q^2} dm^2. \quad (6)$$

The pieces from the large circle C_R on the two sides of the equation have canceled. The distinction between the lower bounds m_F^2 and m_f^2 forces $\text{Im}\Pi(m^2)$ to deviate from $\text{Im}\Pi^P(m^2)$ under the above dispersion relation. Moving the integrand on the right-hand side to the left-hand side, and regarding it as a subtraction term, we attain

$$\int_{m_f^2}^{\infty} \frac{\Delta\rho(m^2)}{m_Q^2 - m^2} dm^2 = 0. \quad (7)$$

The subtracted unknown function $\Delta\rho(m^2) \equiv \text{Im}\Pi(m^2) - \text{Im}\Pi^P(m^2)$ is set to $-\text{Im}\Pi^P(m^2)$ in the interval (m_f^2, m_F^2) of the variable m^2 as an initial condition, and approaches zero at large m^2 , owing to $\text{Im}\Pi(m^2) \rightarrow \text{Im}\Pi^P(m^2)$ in this limit. Accordingly, the radius R of the large circle has been extended to infinity. Since Eq. (7) holds for any large m_Q , it imposes a strict connection between the nonperturbative behavior of $\text{Im}\Pi(m^2)$ near the threshold and the perturbative $\text{Im}\Pi^P(m^2)$.

The variable changes $m_Q^2 - m_f^2 = u\Lambda$ and $m^2 - m_f^2 = v\Lambda$, Λ being an arbitrary scale, turn Eq. (7) into

$$\int_0^{\infty} dv \frac{\Delta\rho(v)}{u - v} = 0. \quad (8)$$

The arbitrariness of the radius R in Eq. (6) has been switched to that of the scale Λ in some sense. We request that $\Delta\rho(v)$ diminishes quickly (to be precise, exponentially) at large v ; namely, $\text{Im}\Pi(m^2)$ approaches $\text{Im}\Pi^P(m^2)$ quickly at large m^2 . The fast diminishing of $\Delta\rho(v)$ at high v is one of the boundary conditions for solving the above integral equation (another is specified in the low end of v , i.e., in the interval $(0, (m_F^2 - m_f^2)/\Lambda)$ below). The major contribution to Eq. (8) then arises from the region with finite v , such that Eq. (8) can be expanded into a power series in $1/u$ for sufficiently large u by inserting $1/(u - v) = \sum_{k=1}^{\infty} v^{k-1}/u^k$. Equation (8) thus demands a vanishing coefficient for every power of $1/u$ on account of the arbitrariness of u , from which a solution can be built up. This method for

solving an integral equation has a solid ground in mathematics, as sketched in [22]. The setup has been applied to the explanation of light fermion and electroweak boson masses successfully [1, 2].

We start with the case with N vanishing coefficients,

$$\int_0^\infty dv v^{k-1} \Delta\rho(v) = 0, \quad k = 1, 2, 3 \cdots, N, \quad (9)$$

where N will be sent to infinity eventually. The first N generalized Laguerre polynomials $L_0^{(\alpha)}(v)$, $L_1^{(\alpha)}(v)$, \dots , $L_{N-1}^{(\alpha)}(v)$ are composed of the terms $1, v, \dots, v^{N-1}$ appearing in the above expressions. Therefore, Eq. (9) implies an expansion of $\Delta\rho(v)$ in $L_k^{(\alpha)}(v)$ with degrees k not lower than N ,

$$\Delta\rho(v) = \sum_{k=N}^{N'} a_k v^\alpha e^{-v} L_k^{(\alpha)}(v), \quad N' > N, \quad (10)$$

attributed to the orthogonality of the polynomials, in which a_k represent a set of unknown coefficients. The index α characterizes the behavior of $\Delta\rho(v)$ around the boundary $v \sim 0$. The highest degree N' can be fixed in principle by the initial condition $-\text{Im}\Pi^{\text{P}}(v)$ of $\Delta\rho(v)$ in the interval $(0, (m_F^2 - m_f^2)/\Lambda)$ of v . Because $-\text{Im}\Pi^{\text{P}}(v)$ is a smooth function, N' needs not be infinite. As proved in [8], the integral equation in Eq. (8) with specified boundary conditions, i.e., the so-called Fredholm equation of the first kind, has a unique solution, which describes the properties of $\Delta\rho(v)$ in the whole range of v .

A generalized Laguerre polynomial takes the asymptotic form for large k , $L_k^{(\alpha)}(v) \approx k^{\alpha/2} v^{-\alpha/2} e^{v/2} J_\alpha(2\sqrt{kv})$ [23], up to corrections of $O(1/\sqrt{k})$ with J_α being a Bessel function. Equation (10) becomes

$$\Delta\rho(m^2) \approx \sum_{k=N}^{N'} a_k \sqrt{\frac{k(m^2 - m_f^2)}{\Lambda}}^\alpha e^{-(m^2 - m_f^2)/(2\Lambda)} J_\alpha \left(2\sqrt{\frac{k(m^2 - m_f^2)}{\Lambda}} \right), \quad (11)$$

where the argument $m^2 = v\Lambda + m_f^2$ has been recovered. Defining the scaling variable $\omega \equiv \sqrt{N/\Lambda}$, we have the approximation $N'/\Lambda = \omega^2[1 + (N' - N)/N] \approx \omega^2$ for finite $N' - N$. The common Bessel functions $J_\alpha \left(2\sqrt{k(m^2 - m_f^2)/\Lambda} \right) \approx J_\alpha \left(2\omega\sqrt{m^2 - m_f^2} \right)$ for $k = N, N+1, \dots, N'$ can then be factored out, such that the unknown coefficients are summed into a single parameter $a = \sum_{k=N}^{N'} a_k$. It has been verified [1, 2, 5] that a single ($N' = N$) Bessel function J_α can fit the initial condition in the interval (m_f^2, m_F^2) well. The arbitrariness of Λ , tracing back to that of the radius R , goes into the variable ω . We are permitted to treat ω as a finite quantity, though both N and Λ are very large. The exponential suppression factor $e^{-(m^2 - m_f^2)/(2\Lambda)} = e^{-\omega^2(m^2 - m_f^2)/(2N)}$ in Eq. (11) is further replaced by unity for finite ω and high N .

We establish the solution to the integral equation in Eq. (7),

$$\Delta\rho(m_Q^2) \approx a \left(\omega\sqrt{m_Q^2 - m_f^2} \right)^\alpha J_\alpha \left(2\omega\sqrt{m_Q^2 - m_f^2} \right), \quad (12)$$

whose parameters can be determined by the boundary conditions. First, Eq. (12) scales in the threshold region with $m_Q \sim m_f$ like $\Delta\rho(m_Q^2) \propto (m_Q^2 - m_f^2)^\alpha$ according to the approximation $J_\alpha(z) \propto z^\alpha$ in the limit $z \rightarrow 0$. Contrasting this scaling law near the threshold with that of the initial condition $-\text{Im}\Pi^{\text{P}}(m_Q^2)$, we read off the index α . Another condition $\Delta\rho(m_F^2) = -\text{Im}\Pi^{\text{P}}(m_F^2)$ at $m_Q = m_F$ sets the overall coefficient

$$a = -\text{Im}\Pi^{\text{P}}(m_F^2) \left[\left(\omega\sqrt{m_F^2 - m_f^2} \right)^\alpha J_\alpha \left(2\omega\sqrt{m_F^2 - m_f^2} \right) \right]^{-1}. \quad (13)$$

A solution for the physical decay width must be insensitive to the arbitrary variable ω . To realize this insensitivity, we make a Taylor expansion of $\Delta\rho(m_Q^2)$ [2],

$$\Delta\rho(m_Q^2) = \Delta\rho(m_Q^2)|_{\omega=\bar{\omega}} + \frac{d\Delta\rho(m_Q^2)}{d\omega} \Big|_{\omega=\bar{\omega}} (\omega - \bar{\omega}) + \frac{1}{2} \frac{d^2\Delta\rho(m_Q^2)}{d\omega^2} \Big|_{\omega=\bar{\omega}} (\omega - \bar{\omega})^2 + \dots, \quad (14)$$

where the constant $\bar{\omega}$, together with the index α and the coefficient a , are fixed through the fit of the first term $\Delta\rho(m_Q^2)|_{\omega=\bar{\omega}}$ to the initial condition in the interval (m_f^2, m_F^2) of m_Q^2 . The insensitivity to the scaling variable ω is

achieved by vanishing the first derivative in Eq. (14),

$$\left. \frac{d\Delta\rho(m_Q^2)}{d\omega} \right|_{\omega=\bar{\omega}} = 0, \quad (15)$$

from which roots of m_Q are solved. Moreover, the second derivative $d^2\Delta\rho(m_Q^2)/d\omega^2|_{\omega=\bar{\omega}}$ needs to be minimal to maximize the stability window around $\bar{\omega}$, in which $\Delta\rho(m_Q^2)$ is almost independent of the variation of ω . As a consequence, only when m_Q takes a specific value, can the above requirements be met. Once a solution is constructed, the degree N for the polynomial expansion in Eq. (10) and the scale Λ can approach infinity by maintaining $\omega = \sqrt{N/\Lambda}$ within the stability window. Then all the arguments based on the large N assumption, including the neglect of the exponential factor $e^{-(m^2-m_f^2)/(2\Lambda)}$ in Eq. (11), are justified.

III. MASSES OF THE FOURTH GENERATION LEPTONS

We apply the formalism outlined in the previous section to the analyses of the $t \rightarrow de^+\nu_4$, $L^- \rightarrow \nu_1\bar{t}d$ and $L^- \rightarrow \nu_4\bar{u}d$ decay widths, and determine the masses m_4 and m_L of the fourth generation leptons.

A. m_4 from the $t \rightarrow de^+\nu_4$ Decay

Since a CKM matrix element can vary independently in a mathematical point of view, heavy quark decays with different CKM matrix elements, i.e., into distinct final states, follow separate dispersion relations. It is thus legitimate to acquire a fermion mass by analyzing appropriate modes. The application to the semileptonic decay $b \rightarrow u\tau^-\bar{\nu}_\tau$, τ (ν_τ) being a τ lepton (neutrino), has generated the expected b quark mass $m_b \approx 4$ GeV, given the τ lepton mass $m_\tau \approx 2$ GeV [1]. It was pointed out in the Introduction that the fourth generation leptons are heavier than half of the Z boson mass. We attempt the scenario that the fourth generation neutrino ν_4 is lighter than the charged lepton L and than a top quark, and constrain its mass m_4 using the $t \rightarrow de^+\nu_4$ decay width. The mass m_4 is identified as the one, which reproduces the top quark mass $m_t \approx 173$ GeV [9] from the corresponding dispersion relation. This strategy is analogous to the one adopted for the $b \rightarrow u\tau^-\bar{\nu}_\tau$ decay [1]. The ordering of m_4 , m_t and m_L will be confirmed at the end of this section.

The width of the semileptonic decay $t \rightarrow bW^+ \rightarrow b\ell^+\nu_\ell$ has been obtained in [24] up to the $O(\alpha_s)$ correction with the strong coupling constant α_s [25]. For related higher-order QCD calculations of the $t \rightarrow bW$ decay width, refer to the recent publication [26]. We first deduce the tree-level expression for the $t \rightarrow de^+\nu_4$ decay width from the formulas in [27], and then incorporate the $O(\alpha_s)$ correction [25], where the m_b -dependent terms are removed to match the considered mode with a massless down quark. Define the energy fraction $x_e = 2E_e/m_t$ of the positron e^+ and the dimensionless variable $y_W = q^2/m_t^2$, q^2 being the invariant mass squared of the W boson, i.e., the $e^+\nu_4$ pair. It is trivial to specify their kinematic ranges

$$\begin{aligned} 0 &\leq x_e \leq 1 - \eta, \\ \eta \left(1 + \frac{x_e}{1 - x_e} \right) &\leq y_W \leq x_e + \eta, \end{aligned} \quad (16)$$

with the notation $\eta = m_4^2/m_t^2$. The involved hard kernel is proportional to [27]

$$(p_t \cdot p_e)(p_d \cdot p_{\nu_4}) \propto x_e(1 - \eta - x_e), \quad (17)$$

where p_t (p_e , p_d , p_{ν_4}) is the momentum of the top quark t (the positron e^+ , the down quark d , the heavy neutrino ν_4).

The $t \rightarrow de^+\nu_4$ decay width from the perturbative evaluation is then written as

$$\Gamma^{\text{P}}(m_t) \propto G_F^2 m_t^5 (1 - \eta)^4 \int_0^1 dx x \int_0^1 \frac{m_W^4 dy}{[m_W^2 - m_t^2 y_W(x, y)]^2 + \Gamma_W^4} \left[(1 - \eta)x(1 - x) - \frac{2\alpha_s(m_t)}{3\pi} F_t(x) \right], \quad (18)$$

with m_W (Γ_W) being the mass (width) of a W boson. The overall constant coefficient, including the Fermi constant G_F , the CKM matrix element V_{td} and the PMNS matrix element U_{e4} , is not crucial, in that it is canceled from the two sides of Eq. (6). The range of the integration variable x has been scaled into $[0, 1]$ via $x_e = (1 - \eta)x$. The effective weak Hamiltonian with the W boson mass being integrated out was employed in the studies of bottom or charm

quark decays [1]. Here we need to retain a W boson propagator, which gives rise to the denominator in Eq. (18). The W boson invariant mass squared is expressed, in terms of y_W , as

$$y_W(x, y) = (1 - \eta)^2 x \left(y + \frac{\eta}{1 - \eta} \right) + \eta, \quad (19)$$

which can be regarded as a variable change from y_W to y . The argument of the running coupling constant has been set to $\mu = m_t$. The function collecting the QCD correction reads [25]

$$F_t(x, y) \approx (1 - \eta)x(1 - x) \ln^2[(1 - \eta)(1 - x)] + \frac{5}{2}(1 - x) \ln[(1 - \eta)(1 - x)], \quad (20)$$

where only the dominant threshold logarithmic terms are taken into account. It has been verified that keeping the other $O(\alpha_s)$ pieces changes our prediction for m_4 by less than 1%.

We treat the top quark mass m_t as a variable m_Q and set the perturbative threshold m_f to m_4 in this case (both d and e^+ are massless) as implementing the formalism. Equation (18) behaves, around $m_Q \sim m_f$, like

$$\Gamma^{\text{P}}(m_Q) \propto \frac{(m_Q^2 - m_f^2)^4}{m_Q^3}, \quad (21)$$

which motivates the choice of the integrands in Eq. (6) [2],

$$\text{Im}\Pi^{(\text{P})}(m^2) = \frac{m^3 \Gamma^{(\text{P})}(m)}{(m^2 - m_f^2)^2}. \quad (22)$$

The above expression with a power of m in the numerator suppresses potential residues in the low m region, including that from the pole at $m^2 = m_f^2$, relative to $m^2 = m_Q^2$ at large m_Q . The denominator alleviates the enhancement caused by the modified numerator at large m . The integrands in Eq. (22), as even functions of the variable m , approves the derivation of the dispersion relation starting with Eq. (3). Equations (21) and (22) then prescribe the boundary condition of the subtracted unknown function in the limit $m_Q \rightarrow m_f$,

$$\Delta\rho(m_Q^2) \propto (m_Q^2 - m_f^2)^2. \quad (23)$$

Comparing the scaling law of Eq. (12), $\Delta\rho(m_Q^2) \propto (m_Q^2 - m_f^2)^\alpha$, with Eq. (23), we designate the index $\alpha = 2$; the integrands in Eq. (22) make the input in Eq. (23) proportional to a simple power of $m_Q^2 - m_f^2$, such that the index α can be read off straightforwardly.

The strong coupling constant is given by

$$\alpha_s(\mu) = \frac{4\pi}{\beta_0 \ln(\mu^2/\Lambda_{\text{QCD}}^2)}, \quad (24)$$

with the coefficient $\beta_0 = 11 - 2n_f/3$. We take the QCD scale parameter $\Lambda_{\text{QCD}} = 0.207$ GeV for the number of active quarks $n_f = 5$ [28]. The interval, in which the initial condition is defined, spans from the lower bound $m_f = m_4$ to the upper bound $m_F = m_4 + m_{\pi^0}$, because a π^0 meson is the lightest one among the hadronic bound states formed by a down quark. Inputting $\Gamma_W = 2.085$ GeV, $m_W = 80.4$ GeV, $m_{\pi^0} = 0.135$ GeV [9] and $m_4 = 170$ GeV, we get the parameter $\bar{\omega} = 0.1001$ GeV $^{-1}$ from the best fit of $\Delta\rho(m_Q^2)|_{\omega=\bar{\omega}}$ in Eq. (14), with $\Delta\rho(m_Q^2)$ in Eq. (12), to $-\text{Im}\Pi^{\text{P}}(m_Q^2)$ in Eq. (22), with $\Gamma^{\text{P}}(m_Q)$ in Eq. (18), in the interval (m_f^2, m_F^2) . As seen shortly, this value of m_4 , above half of a Z boson mass, yields the top quark mass $m_t \approx 173$ GeV. The fit quality is as good as that exhibited in [1, 5], and will not be displayed explicitly. The subtracted unknown function $\Delta\rho(m_Q^2)$ shows an oscillatory behavior in m_Q , also similar to what was observed in [1, 5].

Complying with Eq. (15), we work on the derivative

$$D(m_Q) \equiv \frac{d}{d\omega} \frac{J_\alpha \left(2\omega \sqrt{m_Q^2 - m_f^2} \right)}{J_\alpha \left(2\omega \sqrt{m_F^2 - m_f^2} \right)} \Big|_{\omega=\bar{\omega}}, \quad (25)$$

where the factors independent of ω have been dropped. The dependence of $D(m_Q)$ on $m_Q \geq m_F$ plotted in Fig. 2(a) indicates the existence of multiple roots for $D(m_Q) = 0$. It has been checked that the second derivatives are larger at higher roots [1], so smaller roots are preferred in order to maximize the stability window in ω . Figure 2(a) reveals that

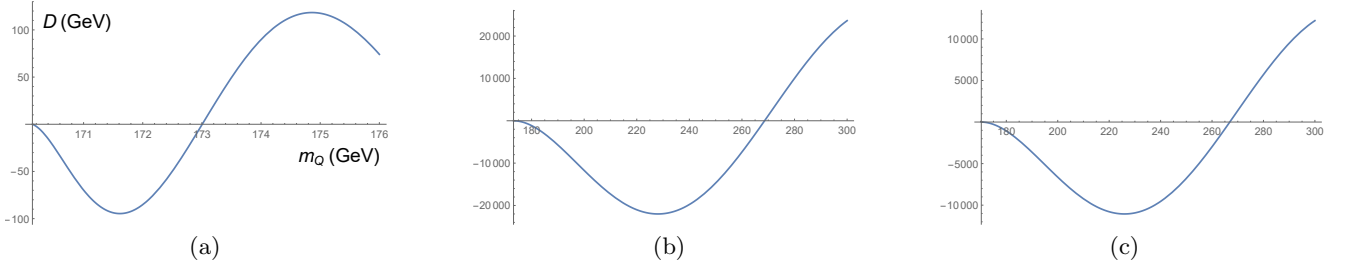


FIG. 2: Dependencies of $D(m_Q)$ in Eq. (25) on m_Q for (a) the $t \rightarrow de^+\nu_4$ decay with $m_4 = 170$ GeV, (b) the $L^- \rightarrow \nu_1 \bar{t} d$ decay with $m_t = 173$ GeV, and (c) the $L^- \rightarrow \nu_4 \bar{u} d$ decay with $m_4 = 170$ GeV.

the derivative first vanishes at $m_Q \approx 173$ GeV above the boundary $m_Q = m_F$. Namely, $m_4 \approx 170$ GeV, leading to $m_t \approx 173$ GeV in the dispersive analysis of the $t \rightarrow de^+\nu_4$ decay, can be identified as the mass the fourth generation neutrino.

The uncertainties from the variations of the top quark mass [9] and of the scale μ within $[m_Q/2, 2m_Q]$ for the coupling constant in Eq. (24) are negligible; they cause less than 1% error, comparable to the amount from the neglect of the $O(\alpha_s)$ constant pieces in Eq. (20). The small error means that our result is robust against the scale changes and higher-order effects, owing to the large threshold mass m_f . The dispersive approach itself also bears theoretical uncertainties, which mainly arise from the large N assumption. Under this assumption the solution in Eq. (12) is approximated by a single Bessel function, so that the determination of the parameter $\bar{\omega}$ from the fit to the initial condition involves some uncertainty. We estimate the impact of this uncertainty by adopting an alternative way to fix $\bar{\omega}$, e.g., by fitting the solution to the initial condition at the midpoint $m_Q^2 = (m_f^2 + m_F^2)/2$ of the interval (m_f^2, m_F^2) . A different value $\bar{\omega} = 0.1079$ is obtained, which changes the prediction for m_4 by less than 1%. In view of the top quark decay width $\Gamma_t = 1.42^{+0.19}_{-0.15}$ GeV [9], the choice of the active quark number $n_f = 6$ and the corresponding QCD scale parameter $\Lambda_{\text{QCD}} = 0.109$ GeV [5, 29] is acceptable. We have tested this set of parameters, and find no effect on the result of m_4 .

B. m_L from the $L^- \rightarrow \nu_1 \bar{t} d$ Decay

The mass $m_4 \approx 170$ GeV of the fourth generation neutrino suggests that the fourth generation charged lepton L may be heavier than a top quark, allowing the determination of its mass m_L from the dispersion relation for the $L^- \rightarrow \nu_1 W^- \rightarrow \nu_1 \bar{t} d$ decay with the input $m_t \approx 173$ GeV. The construction of the $L^- \rightarrow \nu_1 \bar{t} d$ decay width is similar to that of the $t \rightarrow de^+\nu_4$ decay in the previous subsection; we compute the tree-level decay width [27], and then attach the QCD corrections to the $W^- \rightarrow \bar{t} d$ decay, which are available in the literature [30–35]. The energy fraction $x_d \equiv 2E_d/m_L$ of the down quark and the dimensionless variable $y_W \equiv q^2/m_L^2$ from the invariant mass squared of the $\bar{t} d$ pair, i.e., of the W boson, have the ranges the same as in Eq. (16), but with the notation $\eta = m_t^2/m_L^2$. The hard kernel is proportional to

$$(p_L \cdot p_t)(p_d \cdot p_{\nu_1}) \propto (1 + y_W - x_d)(x_d - y_W + \eta), \quad (26)$$

where p_L (p_t , p_{ν_1}) labels the momentum of the heavy lepton L (the anti-top quark \bar{t} , the light neutrino ν_1).

The resultant $L^- \rightarrow \nu_1 \bar{t} d$ decay width is written as

$$\begin{aligned} \Gamma^{\text{P}}(m_L) &\propto G_F^2 m_L^5 (1 - \eta)^3 \int_0^1 dx x \int_0^1 dy \frac{m_W^4 [1 + y_W(x, y) - (1 - \eta)x][(1 - \eta)x - y_W(x, y) + \eta]}{[m_W^2 - m_L^2 y_W(x, y)]^2 + \Gamma_W^4} \\ &\times \left[1 + \frac{\alpha_s(m_L)}{\pi} + \frac{\alpha_s^2(m_L)}{\pi^2} F_W^{(2)}(x, y) + \frac{\alpha_s^3(m_L)}{\pi^3} F_W^{(3)}(x, y) \right], \end{aligned} \quad (27)$$

with x being introduced by the variable change $x_d = (1 - \eta)x$ and the expression of y_W identical to Eq. (19). The argument of the running coupling constant has been set to $\mu = m_L$. The $O(\alpha_s^2)$ and $O(\alpha_s^3)$ corrections read [34]

$$\begin{aligned} F_W^{(2)}(x, y) &= \frac{365}{24} - 11\zeta(3) + n_f \left[\frac{2}{3}\zeta(3) - \frac{11}{12} \right] + \left(\frac{n_f}{6} - \frac{11}{4} \right) \ln[y_W(x, y)], \\ F_W^{(3)}(x, y) &= n_f^2 \left[\frac{2}{9}\zeta(3) - \frac{11}{36} \right] \ln[y_W(x, y)] + \frac{n_f^2}{36} \ln^2[y_W(x, y)], \end{aligned} \quad (28)$$

where $\zeta(3)$ denotes the value of the Riemann zeta function $\zeta(z)$ at $z = 3$, and only the dominant logarithmic terms with the enhancement of n_f^2 are kept in the latter for simplicity. We point out that the $O(\alpha_s^3)$ piece is not important here, since the invariant mass of the $\bar{t}d$ pair must be above the top quark mass. Nevertheless, we include it for the $L^- \rightarrow \nu_4 \bar{u}d$ decay to be investigated in the next subsection, where the $\bar{u}d$ quark pair can be generated with a low invariant mass.

We regard the heavy lepton mass m_L as a variable m_Q , set the quark-level threshold $m_f = m_t$, and choose the integrands in Eq. (6) as

$$\text{Im}\Pi^{(p)}(m^2) = \frac{m^5 \Gamma^{(p)}(m)}{(m^2 - m_f^2)^3}, \quad (29)$$

according to the behavior of Eq. (27) in the region with $m_Q \sim m_f$,

$$\Gamma^p(m_Q) \propto \frac{(m_Q^2 - m_f^2)^5}{m_Q^5}. \quad (30)$$

Equations (29) and (30) together fix the initial condition of the subtracted unknown function in the limit $m_Q \rightarrow m_f$,

$$\Delta\rho(m_Q^2) \propto (m_Q^2 - m_f^2)^2, \quad (31)$$

and the index $\alpha = 2$ in Eq. (12). With the QCD scale parameter $\Lambda_{\text{QCD}} = 0.109$ GeV for the active quark number $n_f = 6$ in Eq. (24), we attain the parameter $\bar{\omega} = 0.0155$ GeV $^{-1}$ from the fit of $\Delta\rho(m_Q^2)|_{\omega=\bar{\omega}}$ to the initial condition $-\text{Im}\Pi^p(m_Q^2)$ in the interval (m_f^2, m_F^2) , $m_F = m_t + m_{\pi^0}$ being the hadronic threshold.

The dependence of the derivative $D(m_Q)$ in Eq. (25) on m_Q for $\alpha = 2$ and $\bar{\omega} = 0.0155$ GeV $^{-1}$ is presented in Fig. 2(b), where the first root, to be identified as the heavy lepton mass m_L , appears at $m_Q \approx 269$ GeV. Varying the top quark mass [9] and the scale μ for $\alpha_s(\mu)$ within the range $[m_Q/2, 2m_Q]$ produces only 1% uncertainty. The uncertainty from the theoretical framework, as estimated in the previous subsection, is also found to be about 1%. The mass of a sequential heavy charged lepton roughly below 100 GeV has been excluded at 95% CL via measurements of the $L \rightarrow \nu W$ decays [9]. It was proposed to detect heavy charged lepton pairs in a Drell-Yan process at LHC [36], whose production rate at $m_L \approx 270$ GeV is about 10^{-3} lower than the top pair one due to the suppression from the coupling constant and parton distribution functions.

C. Cross-check by the $L^- \rightarrow \nu_4 \bar{u}d$ Decay

We corroborate that the masses of the fourth generation leptons predicted in the previous subsections satisfy the dispersion relation for the $L^- \rightarrow \nu_4 W^- \rightarrow \nu_4 \bar{u}d$ decay. The associated formula can also be derived by combining the tree-level $L^- \rightarrow \nu_4 \bar{u}d$ decay width and the QCD corrections to the $W^- \rightarrow \bar{u}d$ decay width up to three loops [34]. The expression is simpler, as the energy fraction is assigned to the \bar{u} quark with $x_u \equiv 2E_u/m_L$, whose range is the same as in Eq. (16). The variable $y_W \equiv q^2/m_L^2$, representing the invariant mass squared of the $\bar{u}d$ pair, takes values within

$$0 \leq y_W \leq \frac{x_u(1 - \eta - x_u)}{1 - x_u}, \quad (32)$$

for the notation $\eta = m_4^2/m_L^2$. The hard kernel is analogous to Eq. (17),

$$(p_L \cdot p_u)(p_d \cdot p_{\nu_4}) \propto x_u(1 - \eta - x_u), \quad (33)$$

with the momentum p_u of the \bar{u} quark.

The $L^- \rightarrow \nu_4 \bar{u}d$ decay width is given, in a perturbation theory, by

$$\begin{aligned} \Gamma^p &\propto G_F^2 m_L^5 (1 - \eta)^5 \int_0^1 dx \frac{x^2(1-x)^2}{1 - (1-\eta)x} \int_0^1 \frac{m_W^4 dy}{[m_W^2 - m_L^2 y_W(x, y)]^2 + \Gamma_W^4} \\ &\times \left[1 + \frac{\alpha_s(m_L)}{\pi} + \frac{\alpha_s^2(m_L)}{\pi^2} F_W^{(2)}(x, y) + \frac{\alpha_s^3(m_L)}{\pi^3} F_W^{(3)}(x, y) \right], \end{aligned} \quad (34)$$

where the variable x is related to x_u via $x_u = (1 - \eta)x$, and the function

$$y_W(x, y) = \frac{(1 - \eta)^2 x(1 - x)}{1 - (1 - \eta)x}, \quad (35)$$

serves as a variable change from y_W to y . The $O(\alpha_s^2)$ and $O(\alpha_s^3)$ corrections, $F_W^{(2)}(x, y)$ and $F_W^{(3)}(x, y)$, have been defined in Eq. (28).

Equation (34) behaves like Eq. (30) in the threshold region with $m_Q \sim m_f = m_4$, so the integrands in Eq. (6) follow Eq. (29). We then have the initial condition of the subtracted unknown function in Eq. (31) in the limit $m_Q \rightarrow m_f$, and the index $\alpha = 2$ for Eq. (12). The parameter $\bar{\omega} = 0.0155 \text{ GeV}^{-1}$ is drawn from the fit of $\Delta\rho(m_Q^2)|_{\omega=\bar{\omega}}$ to the initial condition in the interval (m_f^2, m_F^2) , where the upper bound is chosen as $m_F = m_4 + m_{\pi^0} + m_{\pi^-}$, with $n_f = 6$ and $\Lambda_{\text{QCD}} = 0.109 \text{ GeV}$ in Eq. (24) and the inputs $m_4 = 170 \text{ GeV}$ and $m_{\pi^-} = 0.140 \text{ GeV}$ [9]. The dependence of the derivative $D(m_Q)$ in Eq. (25) on m_Q for $\alpha = 2$ and $\bar{\omega} = 0.0155 \text{ GeV}^{-1}$ is shown in Fig. 2(c), where the first root located at $m_Q \approx 267 \text{ GeV}$ is identified as the heavy lepton mass m_L . This value is very close to $m_L \approx 269 \text{ GeV}$ in the previous subsection with deviation less than 1%. The concordance between the analyses of different modes supports the consistency of our formalism and the predictions for the fourth generation lepton masses. The variation of the scale μ for $\alpha_s(\mu)$ is the major source of the theoretical uncertainty, resulting in $m_L \approx 248 \text{ GeV}$ for $\mu = m_Q/2$ and $m_L \approx 289 \text{ GeV}$ for $\mu = 2m_Q$, i.e., $m_L \approx (267 \pm 20) \text{ GeV}$. The sensitivity originates from the lower invariant mass that the $\bar{u}d$ quark pair can reach as mentioned before, and from the resultant enhancement of the radiative logarithmic corrections. The uncertainty from the theoretical framework may amount to 6% in this decay channel. It is noticed that the neglect of the $O(\alpha_s^3)$ piece $F_W^{(3)}$ would increase the result of m_L by 20%. It highlights the relevance of this higher-order contribution here, contrary to the $L^- \rightarrow \nu_1 \bar{t}d$ case.

IV. EXPERIMENTAL CONSTRAINTS ON THE FOURTH-GENERATION LEPTONS

The experimental bounds on the parameters in the sequential fourth generation model have been surveyed in the literature. Our predictions for $m_4 \approx 170 \text{ GeV}$ and $m_L \approx 270 \text{ GeV}$, and for their mass splitting accommodate the fit results in [37], but are higher than $m_4 = 58.0 \text{ GeV}$ and $m_L = 113.6 \text{ GeV}$ from [38], which assumed lighter fourth generation quarks of masses about 600 GeV. Unlike the fourth generation quarks with masses above a TeV scale [5], the fourth generation leptons do not form bound states in a Yukawa potential. Though they are not involved in the Higgs production via gluon fusion, the charged lepton contributes to the Higgs decay into a photon pair, $H \rightarrow \gamma\gamma$. Therefore, the argument for the fourth generation quarks to bypass the experimental constraints from the Higgs decay by means of the formation of bound states [5] does not apply. It is necessary to scrutinize whether the Higgs decay data rule out the existence of the fourth generation charged lepton.

The $H \rightarrow \gamma\gamma$ decay width with the contribution from the fourth generation charged lepton is expressed as [39]

$$\Gamma_{\gamma\gamma} = \frac{\alpha_e^2 G_F m_H^3}{128\sqrt{2}\pi^3} |J_{\gamma\gamma}|^2, \quad (36)$$

where α_e is the fine structure constant and m_H the Higgs mass. The decay amplitude contains three terms,

$$J_{\gamma\gamma} = \left(\frac{2}{3}\right)^2 N_c I(r_t) + I(r_L) + K(r_W), \quad (37)$$

with the functions

$$\begin{aligned} I(x) &= \frac{2}{x^2} [x + (x-1)f(x)], & K(x) &= - \left[2 + \frac{3}{x} + \frac{3}{x^2} (2x-1)f(x) \right], \\ f(x) &= \arcsin^2 \sqrt{x}. \end{aligned} \quad (38)$$

Inserting $r_{t,L,W} = m_H^2/(4m_{t,L,W}^2)$ with $m_H = 125 \text{ GeV}$, $m_t = 173 \text{ GeV}$, $m_L = 270 \text{ GeV}$ and $m_W = 80.4 \text{ GeV}$, we obtain the ratio

$$\frac{|J_{\gamma\gamma}|^2}{|J_{\gamma\gamma}^{\text{SM}}|^2} = 0.63, \quad (39)$$

where $J_{\gamma\gamma}^{\text{SM}}$ comes from Eq. (37) but without the $I(r_L)$ piece. That is, $\Gamma_{\gamma\gamma}$ is reduced by 37%; the terms from fermion loops in Eq. (37) are destructive to the dominant one from a W -boson loop, so the fourth generation charged lepton decreases the decay width.

The recent calculation for the above width, which takes into account various sources of subleading corrections in the SM, gives $\Gamma_{\gamma\gamma}^{\text{SM}} = (9.28 \pm 0.16) \times 10^{-6} \text{ GeV}$ [40]. The theoretical uncertainty covers those from QCD contributions, electroweak contributions and variations of input parameters. We mention another result $\Gamma_{\gamma\gamma}^{\text{SM}} \approx 9.4 \times 10^{-6} \text{ GeV}$

with similar precision [41]. As to the data, we estimate $\Gamma_{\gamma\gamma}^{\text{data}} \approx (9.3_{-3.5}^{+4.8}) \times 10^{-3}$ MeV from the width $3.7_{-1.4}^{+1.9}$ MeV of a Higgs boson and the measured $H \rightarrow \gamma\gamma$ branching ratio $(2.50 \pm 0.20) \times 10^{-3}$ [9], where the small error from the branching ratio has been ignored. Hence, the 37% deduction of the SM prediction [40], i.e., the modified width $\Gamma_{\gamma\gamma} = (5.85 \pm 0.10) \times 10^{-3}$ MeV still agrees with the data within the experimental uncertainty. We postulate that the Higgs decay data does not exclude the existence of the fourth generation charged lepton.

Together with the masses of the fourth generation quarks predicted in [5], we are ready to address the fourth generation contributions to the oblique parameters S , T and U . It has been known that the superheavy fourth generation quarks form bound states under a strong Yukawa potential [14, 15]. The oblique parameters are ultraviolet finite and do not probe the internal structure of these bound states, similar to the cases of the Higgs production from gluon fusion and the Higgs decay into a photon pair [5]. Therefore, the contribution to the oblique parameters from the fourth generation quarks can be assessed in the same effective approach as in [5]. The fourth generation leptons are too light to form bound states, so we quantify their impact by adopting the one-loop formulas in [17]. It will be explained in the next section that the mixing of the fourth generation leptons with the other light generations is quite weak, an observation in line with the assumption made in [17]. Substituting $m_4 = 170$ GeV, $m_L = 270$ GeV and the Z boson mass $m_Z = 91.2$ GeV [9] into Eqs. (9)-(11) in [17], we get straightforwardly

$$S = 0.003, \quad T = 0.178, \quad U = 0.009. \quad (40)$$

It is noticed that the fourth generation leptons with the distinct masses m_4 and m_L induce the oblique parameter T more significantly, which measures isospin breaking effects of new physics [42].

Below we estimate the order of magnitude of the contributions from the bound states formed by the fourth generation quarks, and certify that they are much smaller than from the fourth generation leptons. In the viewpoint of an effective theory, the oblique parameters describe the process, where an electroweak boson W turns into a vector boson V , a bound state of the fourth generation quarks, through a dimensionless coupling g_{WV} between them. The vector boson V propagates according to a Breit-Wigner factor $1/(m_V^2 - s - i\sqrt{s}\Gamma_V)$ with the invariant mass squared $s = q^2$, where m_V (Γ_V , q) is the mass (width, momentum) of V . The vector boson V then transforms into another electroweak boson W' with the dimensionless coupling $g_{W'V}$. The corresponding amplitude is thus formulated, in the effective approach, as

$$\frac{g_{WV}g_{W'V}s(g^{\mu\nu} - q^\mu q^\nu/s)}{m_V^2 - s - i\sqrt{s}\Gamma_V}, \quad (41)$$

where factors irrelevant to our reasoning are implicit.

Take the contribution from a $\bar{b}'b'$ bound state to the oblique parameter S as an example. The product of the effective couplings $g_{WV}g_{W'V}$ can be fixed by matching the amplitude in Eq. (41) to the perturbative one $S_{b'}(s)$ in the fundamental theory at a high scale s [17],

$$S_{b'}(s) = \frac{N_c}{6\pi} \left\{ 2(3 - 4Y_{b'}) \frac{m_{b'}^2}{s} + 2Y_{b'} \ln \frac{m_{b'}^2}{s} + \left[\left(\frac{3}{2} - 2Y_{b'} \right) \frac{m_{b'}^2}{s} - Y_{b'} \right] G \left(\frac{m_{b'}^2}{s} \right) \right\}, \quad (42)$$

$$G(x) = -4\sqrt{4x-1} \arctan \frac{1}{\sqrt{4x-1}},$$

$N_c = 3$ being the color number and $Y_{b'} = 1/6$ the hypercharge of a b' quark. Relating Eq. (41) to Eq. (42) at the large mass squared $s \approx m_{b'}^2$, we have

$$\frac{g_{WV}g_{W'V}m_{b'}^2}{m_V^2 - m_{b'}^2} \sim S_{b'}(m_{b'}^2), \quad (43)$$

where the product $m_{b'}\Gamma_V < m_V^2 - m_{b'}^2$ has been neglected in the denominator for $m_V \sim 3$ TeV and $\Gamma_V \sim 500$ GeV from [5]. The above relation then implies $g_{WV}g_{W'V} \sim S_{b'}(m_{b'}^2)(m_V^2/m_{b'}^2 - 1)$.

Extrapolating Eq. (41) to the region with $s \approx m_Z^2 \ll m_{b'}^2$, we obtain the suppression factor on the vector boson contribution relative to the perturbative one $S_{b'}(m_Z^2)$,

$$\frac{g_{WV}g_{W'V}s}{S_{b'}(m_Z^2)(m_V^2 - s)} \approx \frac{S_{b'}(m_{b'}^2)m_Z^2(m_V^2 - m_{b'}^2)}{S_{b'}(m_Z^2)m_{b'}^2m_V^2} \sim 10^{-4}. \quad (44)$$

The exact values of $S_{b'}(m_Z^2)$ and $S_{b'}(m_{b'}^2)$ do not matter actually, for they are of the same order of magnitude, and largely cancel in the above ratio. Equation (44) manifests that the vector contribution decreases like m_Z^2/m_V^2 ($m_{b'}$ and m_V are of the same order of magnitude), and that the $\bar{b}'t'$ and $\bar{t}'t'$ contributions are even more suppressed by huge

vector boson masses. With $S_{b'}(m_Z^2) \approx 0.5$ from Eq. (42), it is easy to see that the $\bar{b}'b'$ contribution is of $O(10^{-5})$, lower than the one from the fourth generation lepton by a factor of 10^{-2} . The same observation applies to the bound-state contributions to the oblique parameters T and U , and will not be repeated here.

We conclude that the contributions from the fourth generation fermions to the oblique parameters are dominated by those from the leptons already given in Eq. (40). The global fits to electroweak precision measurements indicate that new physics effects cause the oblique parameters [9]

$$S = -0.04 \pm 0.10, \quad T = 0.01 \pm 0.12, \quad U = -0.01 \pm 0.09. \quad (45)$$

Equation (40), consistent with the above data within 2σ error, i.e., 95% CL, asserts that the sequential fourth generation model is not ruled out, and deserves further pursuits.

V. CONSTRAINTS ON THE PMNS MATRIX ELEMENTS

We have explored the dispersion relations for the mixing of neutral leptonic states $\mathcal{L}^-\ell^+$ and $\mathcal{L}^+\ell^-$, like μ^-e^+ and μ^+e^- , in [3, 4], where \mathcal{L} (ℓ) stands for a massive (light) charged lepton, and observed that these relations impose strong constraints on the neutrino masses and the PMNS matrix elements. If the fourth generation leptons exist, they might affect the constraints inferred from the three-generation case. The only assumption underlying the analysis is that the electroweak symmetry of the SM is restored at a high energy scale Λ [43, 44], which could be realized in, for instance, the composite Higgs model [45]. It was then argued based on the unitarity of the PMNS matrix that the mixing phenomenon disappears, as the electroweak symmetry of the SM is restored. The disappearance of the mixing at $m_{\mathcal{L}} > \Lambda$ was taken as the input to the dispersion relation, $m_{\mathcal{L}}$ being the mass of the heavy lepton \mathcal{L} , and the solution at low $m_{\mathcal{L}} < \Lambda$, i.e., in the symmetry broken phase, was found to bind the neutrino masses and the PMNS matrix elements involved in the mixing amplitude [3]. We point out that Λ plays a role similar to the large scale in Sec. III, above which perturbative inputs are reliable.

We decompose the mixing amplitude $\Pi(m_Q^2)$ into a sum over various intermediate neutrino channels,

$$\begin{aligned} \Pi(m_{\mathcal{L}}^2) &= M(m_{\mathcal{L}}^2) - \frac{i}{2}\Gamma(m_{\mathcal{L}}^2) \\ &\equiv \sum_{i,j=1}^4 \lambda_i \lambda_j \left[M_{ij}(m_{\mathcal{L}}^2) - \frac{i}{2}\Gamma_{ij}(m_{\mathcal{L}}^2) \right], \end{aligned} \quad (46)$$

where $\lambda_i \equiv U_{\mathcal{L}i}^* U_{\ell i}$ is the product of the 4×4 PMNS matrix elements. It has been elaborated [4] that the dependence of the real part $M_{ij}(m_{\mathcal{L}}^2)$ on the intermediate neutrino masses, i.e., the contribution which survives the summation over all intermediate channels, begins at the three-loop level in the symmetric phase. In other words, the argument on the disappearance of the mixing phenomenon, $\sum_{i,j} \lambda_i \lambda_j M_{ij}(m_{\mathcal{L}}^2) \approx 0$, in the symmetric phase is valid to high accuracy. The corresponding dispersion relation is thus written as

$$M(m_{\mathcal{L}}^2) = \frac{1}{2\pi} \int^{\Lambda^2} dm^2 \frac{\Gamma(m^2)}{m_{\mathcal{L}}^2 - m^2} \approx 0, \quad (47)$$

for $m_{\mathcal{L}} > \Lambda$.

To diminish the dispersive integral in Eq. (47) for arbitrary $m_{\mathcal{L}} > \Lambda$, some conditions must be met by the PMNS matrix elements. We quote the asymptotic behavior of the imaginary part $\Gamma_{ij}(m^2)$ for $m < \Lambda$ [3, 46, 47]

$$\Gamma_{ij}(m^2) \approx \Gamma_{ij}^{(1)} m^2 + \Gamma_{ij}^{(0)} + \frac{\Gamma_{ij}^{(-1)}}{m^2} + \dots, \quad (48)$$

with the coefficients

$$\begin{aligned} \Gamma_{ij}^{(1)} &= \frac{4m_W^4 - 6m_W^2(m_i^2 + m_j^2) + m_i^2 m_j^2}{2(m_W^2 - m_i^2)(m_W^2 - m_j^2)}, \\ \Gamma_{ij}^{(0)} &= -\frac{3(m_i^2 + m_j^2) [4m_W^4 - 4m_W^2(m_i^2 + m_j^2) + m_i^2 m_j^2]}{2(m_W^2 - m_i^2)(m_W^2 - m_j^2)}, \\ \Gamma_{ij}^{(-1)} &= \frac{3(m_i^4 + m_j^4) [4m_W^4 - 2m_W^2(m_i^2 + m_j^2) + m_i^2 m_j^2]}{2(m_W^2 - m_i^2)(m_W^2 - m_j^2)}. \end{aligned} \quad (49)$$

The terms $\Gamma_{ij}^{(n)}$ give contributions to the dispersive integral in Eq. (47), which scale like Λ^4 , Λ^2 and $\ln \Lambda^2$ for $n = 1, 0$ and -1 , respectively. Since Λ just needs to be of order of the symmetry restoration scale, instead of a definite value, it is unlikely that the above huge contributions happen to cancel among themselves. The finiteness of the dispersive integral can only be achieved by requiring

$$\sum_{i,j=1}^4 \lambda_i \lambda_j \Gamma_{ij}^{(n)} \approx 0, \quad n = 1, 0, -1. \quad (50)$$

Once the conditions in Eq. (50) are fulfilled, we recast the dispersive integral in Eq. (47) into

$$\int^{\Lambda^2} dm^2 \frac{\Gamma(m^2)}{m_{\mathcal{L}}^2 - m^2} \approx \frac{1}{m_{\mathcal{L}}^2} \sum_{i,j=1}^4 \lambda_i \lambda_j g_{ij}, \quad (51)$$

with the factors

$$g_{ij} \equiv \int_{t_{ij}}^{\infty} dm^2 \left[\Gamma_{ij}(m^2) - \Gamma_{ij}^{(1)} m^2 - \Gamma_{ij}^{(0)} - \frac{\Gamma_{ij}^{(-1)}}{m^2} \right], \quad (52)$$

and the thresholds $t_{ij} = (m_i + m_j)^2$. The approximation $1/(m_{\mathcal{L}}^2 - m^2) \approx 1/m_{\mathcal{L}}^2$ has been made for large $m_{\mathcal{L}} > \Lambda$, because the integral receives contributions only from finite $m < \Lambda$. The integrand in the square brackets decreases like $1/m^4$, so the upper bound of m^2 in Eq. (52) can be pushed to infinity safely. We place the final condition, labeled by $n = f$,

$$\sum_{i,j=1}^4 \lambda_i \lambda_j g_{ij} \approx 0, \quad (53)$$

to ensure the almost nil dispersive integral. That is, the realization of Eqs. (50) and (53) establishes a solution to the integral equation in Eq. (47).

We employ the unitarity condition to eliminate $\lambda_4 = -\lambda_1 - \lambda_2 - \lambda_3$, and define the ratios of the PMNS matrix elements,

$$r_1 \equiv \frac{U_{\mathcal{L}1}^* U_{e1}}{U_{\mathcal{L}2}^* U_{e2}} \equiv u_1 + iv_1, \quad r_3 \equiv \frac{U_{\mathcal{L}3}^* U_{e3}}{U_{\mathcal{L}2}^* U_{e2}} \equiv u_3 + iv_3, \quad (54)$$

where \mathcal{L} represents either μ or τ , and the unknowns $u_{1,3}$ and $v_{1,3}$ will be constrained below. The $n = 1, 0$ and -1 conditions can be factorized into

$$\left(r_1 \frac{m_4^2 - m_1^2}{m_W^2 - m_1^2} + \frac{m_4^2 - m_2^2}{m_W^2 - m_2^2} + r_3 \frac{m_4^2 - m_3^2}{m_W^2 - m_3^2} \right)^2 \approx 0, \quad (55)$$

$$\left(r_1 \frac{m_4^2 - m_1^2}{m_W^2 - m_1^2} + \frac{m_4^2 - m_2^2}{m_W^2 - m_2^2} + r_3 \frac{m_4^2 - m_3^2}{m_W^2 - m_3^2} \right) \left(r_1 \frac{m_4^2 - m_1^2}{m_W^2 - m_1^2} P_1 + \frac{m_4^2 - m_2^2}{m_W^2 - m_2^2} P_2 + r_3 \frac{m_4^2 - m_3^2}{m_W^2 - m_3^2} P_3 \right) \approx 0, \quad (56)$$

$$\left(r_1 \frac{m_4^2 - m_1^2}{m_W^2 - m_1^2} + \frac{m_4^2 - m_2^2}{m_W^2 - m_2^2} + r_3 \frac{m_4^2 - m_3^2}{m_W^2 - m_3^2} \right) \left(r_1 \frac{m_4^2 - m_1^2}{m_W^2 - m_1^2} Q_1 + \frac{m_4^2 - m_2^2}{m_W^2 - m_2^2} Q_2 + r_3 \frac{m_4^2 - m_3^2}{m_W^2 - m_3^2} Q_3 \right) \approx 0, \quad (57)$$

respectively, with the functions

$$P_i = \frac{m_W^2(m_4^2 + m_i^2) - m_4^2 m_i^2}{m_4^4}$$

$$Q_i = \frac{2m_W^4(m_4^2 + m_i^2) + m_4^2 m_i^2(m_4^2 + m_i^2) - m_W^2(m_4^4 + 3m_4^2 m_i^2 + m_i^4)}{m_4^6}. \quad (58)$$

The above conditions have been presented in terms of dimensionless mass ratios as done in [3].

We observe immediately that Eqs. (55)-(57) can be respected simultaneously by diminishing the common factor

$$r_1 \frac{m_4^2 - m_1^2}{m_W^2 - m_1^2} + \frac{m_4^2 - m_2^2}{m_W^2 - m_2^2} + r_3 \frac{m_4^2 - m_3^2}{m_W^2 - m_3^2} \approx 0, \quad \text{i.e.,} \quad \sum_{i=1}^3 U_{\mathcal{L}i}^* U_{ei} = -U_{\mathcal{L}4}^* U_{e4} \sim O\left(\frac{m_i^2}{m_{4,W}^2}\right). \quad (59)$$

It means that the unitarity of the 3×3 PMNS matrix holds well, up to $O(m_i^2/m_{4,W}^2)$ corrections, when the mass m_4 of the fourth generation neutrino is of order of the W boson mass m_W . In the three-generation case there are only two unknowns u_1 and v_1 [3], and Eq. (59) reduces to

$$r_1 \frac{m_3^2 - m_1^2}{m_W^2 - m_1^2} + \frac{m_3^2 - m_2^2}{m_W^2 - m_2^2} \approx 0, \quad \text{i.e.,} \quad \sum_{i=1}^2 U_{\mathcal{L}i}^* U_{ei} = -U_{\mathcal{L}3}^* U_{e3} \sim O\left(\frac{m_i^2}{m_3^2}\right). \quad (60)$$

Namely, we would have the order-of-magnitude estimate $|U_{\mu 3}^* U_{e3}| \sim \sin \theta_{23} \cos \theta_{13} \sin \theta_{13} \sim m_2^2/m_3^2 \approx 0.03$ for $\mathcal{L} = \mu$, much lower than the measured value 0.11 [9]. The above argument is applicable to the quark mixing, such as the $c\bar{u}-\bar{c}u$ mixing, simply by substituting the quark masses $m_{d,s,b,b'}$ for the neutrino masses $m_{1,2,3,4}$. The unitarity of the 3×3 CKM matrix is then expected to be violated at the level $m_b^2/m_W^2 \approx 10^{-3}$, in agreement with the conclusion from recent global fits to precision measurements in flavor physics [48–50]; in the three-generation case, we would have the order-of-magnitude estimate $V_{cb}^* V_{ub} \sim m_s^2/m_b^2 \approx 6.3 \times 10^{-4}$, much higher than the measured value 1.5×10^{-4} [9]. In this sense, the data for the PMNS and CKM matrix elements have hinted the existence of the sequential fourth generation fermions according to the dispersive constraints.

The $n = f$ condition in Eq. (53) possesses a complicated and lengthy form. To an excellent accuracy, we concentrate on the leading terms of a piece

$$G_{ij} = g_{ij} - g_{i4} - g_{j4} + g_{44}, \quad (61)$$

in the sum over the intermediate channels, which is, after the elimination of λ_4 , expanded in powers of $m_i/m_{4,W}$,

$$G_{ij} \approx \frac{-20m_W^4 m_4^4 + 28m_W^2 m_4^6 - 7m_4^8 + (16m_W^4 m_4^3 - 28m_W^2 m_4^5 + 12m_4^7)(m_i + m_j)}{2(m_W^2 - m_4^2)^2(m_W^2 - m_i^2)(m_W^2 - m_j^2)}. \quad (62)$$

Equation (53) then turns into

$$\sum_{i,j=1}^3 G_{ij} \approx -(20m_W^4 - 28m_W^2 m_4^2 + 7m_4^4)G_0 + (16m_W^4 - 28m_4^2 m_W^2 + 12m_4^4)G_1 \approx 0, \quad (63)$$

$$G_0 = \left(\frac{r_1}{m_W^2 - m_1^2} + \frac{1}{m_W^2 - m_2^2} + \frac{r_3}{m_W^2 - m_3^2} \right)^2, \quad (64)$$

$$G_1 = \left(\frac{r_1}{m_W^2 - m_1^2} + \frac{1}{m_W^2 - m_2^2} + \frac{r_3}{m_W^2 - m_3^2} \right) \left[\frac{r_1 m_1}{m_4(m_W^2 - m_1^2)} + \frac{m_2}{m_4(m_W^2 - m_2^2)} + \frac{r_3 m_3}{m_4(m_W^2 - m_3^2)} \right].$$

Reexpressing the factors P_i in Eq. (58) as

$$P_i \approx \frac{m_W^2}{m_4^2} \left(1 + \frac{m_i^2}{m_4^2} - \frac{m_i^2}{m_4^2} \right), \quad (65)$$

we realize that the $n = 0$ condition represents an $O(m_i^2/m_{4,W}^2)$ correction to the $n = 1$ one. The $n = -1$ condition also appears as an $O(m_i^2/m_{4,W}^2)$ correction to the $n = 1$ one, so both Eqs. (56) and (57) can be dropped in the search for the solutions to the dispersive constraints. A distinction from the three-generation case [3] is that the above power corrections become $O(m_{1,2}^2/m_3^2)$, much greater than $O(m_{1,2}^2/m_{4,W}^2)$, and the $n = 0$ and -1 conditions force nontrivial constraints on the PMNS matrix elements. Apparently, Eq. (63) also represents an $O(m_i^2/m_4^2)$ correction to the $n = 1$ condition in Eq. (55), whose contribution is expected to be negligible. The minimization of the four conditions labeled by $n = 1, 0, -1$ and f was performed numerically by tuning the two unknowns u_1 and v_1 in the three-generation case [3]. We have four unknowns with four constraints from Eqs. (55) and (64) here, which contain real and imaginary parts, so that the solution need to be constructed in a different way.

The real and imaginary parts of Eq. (55) lead to

$$u_1 \frac{m_4^2 - m_1^2}{m_W^2 - m_1^2} + \frac{m_4^2 - m_2^2}{m_W^2 - m_2^2} + u_3 \frac{m_4^2 - m_3^2}{m_W^2 - m_3^2} \approx 0, \quad (66)$$

$$v_1 \frac{m_4^2 - m_1^2}{m_W^2 - m_1^2} + v_3 \frac{m_4^2 - m_3^2}{m_W^2 - m_3^2} \approx 0, \quad (67)$$

from which we derive the expressions for u_1 and v_1 in terms of u_3 and v_3 , respectively. The real and imaginary parts of Eq. (64) are written as

$$G_{1r} \equiv \left(\frac{u_1}{m_W^2 - m_1^2} + \frac{1}{m_W^2 - m_2^2} + \frac{u_3}{m_W^2 - m_3^2} \right) \left[\frac{u_1 m_1}{m_4(m_W^2 - m_1^2)} + \frac{m_2}{m_4(m_W^2 - m_2^2)} + \frac{u_3 m_3}{m_4(m_W^2 - m_3^2)} \right] - \left(\frac{v_1}{m_W^2 - m_1^2} + \frac{v_3}{m_W^2 - m_3^2} \right) \left[\frac{v_1 m_1}{m_4(m_W^2 - m_1^2)} + \frac{v_3 m_3}{m_4(m_W^2 - m_3^2)} \right] \approx 0, \quad (68)$$

$$G_{1i} \equiv \left(\frac{u_1}{m_W^2 - m_1^2} + \frac{1}{m_W^2 - m_2^2} + \frac{u_3}{m_W^2 - m_3^2} \right) \left[\frac{v_1 m_1}{m_4(m_W^2 - m_1^2)} + \frac{v_3 m_3}{m_4(m_W^2 - m_3^2)} \right] + \left[\frac{u_1 m_1}{m_4(m_W^2 - m_1^2)} + \frac{m_2}{m_4(m_W^2 - m_2^2)} + \frac{u_3 m_3}{m_4(m_W^2 - m_3^2)} \right] \left(\frac{v_1}{m_W^2 - m_1^2} + \frac{v_3}{m_W^2 - m_3^2} \right) \approx 0. \quad (69)$$

For a given v_1 , G_{1r} represents a parabola in u_1 , so Eq. (68) specifies two roots of u_1 , which will be assigned as the solutions for the μe and τe mixings separately. On the other hand, G_{1i} describes a straight line, and Eq. (69) gives a single root of u_1 . This root is independent of v_1 , such that no definite value of v_1 can be associated with it to form a solution.

We assume a small first generation mass $m_1^2 = 10^{-6} \text{ eV}^2$ [3], and input m_2 and m_3 from the measured mass-squared differences $\Delta m_{21}^2 \equiv m_2^2 - m_1^2 = (7.50_{-0.20}^{+0.22}) \times 10^{-5} \text{ eV}^2$ and $\Delta m_{31}^2 \equiv m_3^2 - m_1^2 = (2.55_{-0.03}^{+0.02}) \times 10^{-3} \text{ eV}^2$ in the NO scenario [51]. The values of u_1 and v_1 are then chosen to render $|G_{1r}|$ and $|G_{1i}|$ have similar deviation from zero around the two roots of u_1 from Eq. (68). Note that v_1 can be determined only up to a sign as observed in [3]. We obtain

$$r_1 \approx -0.83 - 0.04i, \quad -0.98 + 0.04i, \quad (70)$$

which are insensitive to the variation of m_1 . The sign of v_1 has been assigned in the way that the former (latter) solution corresponds to the μe (τe) mixing. Compared with the ratios $r_1 \approx -1.0 - 0.02i$ ($r_1 \approx -1.0 + 0.02i$) for the μe (τe) mixing derived in the three-generation case [3], the real part increases to about -0.83 (remains similar).

The mixing angles $\theta_{12} = (34.3 \pm 1.0)^\circ$, $\theta_{13} = (8.53_{-0.12}^{+0.13})^\circ$ and $\theta_{23} = (49.26 \pm 0.79)^\circ$, and the CP phase $\delta = (194_{-22}^{+24})^\circ$ from [51], and the set of $\theta_{12} = (33.40_{-0.82}^{+0.80})^\circ$, $\theta_{13} = (8.59_{-0.12}^{+0.13})^\circ$, $\theta_{23} = (42.4_{-0.9}^{+1.0})^\circ$ and $\delta = (223_{-23}^{+32})^\circ$ from [52] yield the measured ratios for the μe mixing

$$\frac{U_{\mu 1}^* U_{e 1}}{U_{\mu 2}^* U_{e 2}} = \begin{cases} -(0.676_{-0.005}^{+0.045}) - (0.072_{-0.113}^{+0.118})i, \\ -(0.786_{-0.046}^{+0.116}) - (0.178_{-0.092}^{+0.094})i, \end{cases} \quad (71)$$

respectively, and for the τe mixing

$$\frac{U_{\tau 1}^* U_{e 1}}{U_{\tau 2}^* U_{e 2}} = \begin{cases} -(1.289_{-0.068}^{+0.008}) + (0.079_{-0.125}^{+0.115})i, \\ -(1.260_{-0.104}^{+0.106}) + (0.284_{-0.134}^{+0.076})i, \end{cases} \quad (72)$$

respectively, where the errors mostly come from the variation of δ . Our predictions in Eq. (70) match the above data within uncertainties, and the sign selection for Eq. (70) is affirmed. The splitting of the real parts in the four-generation case, relative to the degenerate real parts in the three-generation case [3], improves the consistency between the theoretical and experimental results notably.

An alternative comparison with the data is made through the mixing angles and CP phase inferred by the solutions in Eq. (70) for the μe and τe mixings. These parameters can be deduced by minimizing the deviation

$$\sum_{\mathcal{L}=\mu,\tau} \left| \frac{U_{\mathcal{L}1}^* U_{e1}}{U_{\mathcal{L}2}^* U_{e2}} - (u_{\mathcal{L}} + v_{\mathcal{L}}i) \right|, \quad (73)$$

with roughly equal contributions from the two pieces labeled by $\mathcal{L} = \mu, \tau$ for $u_{\mu} = -0.83$, $v_{\mu} = -0.04$, $u_{\tau} = -0.98$ and $v_{\tau} = 0.04$. The reason for considering the minimization is that one cannot find roots of the mixing angles and CP phase, which vanish the two pieces simultaneously. It is observed that the mixing angles θ_{12} and θ_{23} are correlated with each other, and the deviation in Eq. (73) decreases with θ_{12} . However, a large θ_{12} renders the domain for minimal deviation in the θ_{13} - δ plane broad, such that no definite values of θ_{13} and δ can be retrieved. Taking these facts into account, we set $\theta_{12} = 34^\circ$, for which the minimization of Eq. (73) generates

$$\theta_{23} \approx 47^\circ, \quad \theta_{13} \approx 5^\circ, \quad \delta \approx 200^\circ. \quad (74)$$

The above outcomes are stable against the variation of m_1 and, except θ_{13} , do not differ much from the data [51, 52]. The angle θ_{23} is close to the maximal mixing 45° , as concluded in [3], and slightly prefers to be in the second octant. We mention that the two recent global fits lead to different octants for θ_{23} (49.3° vs 42.4°) [51, 52].

The angle θ_{13} , assuming a small value, might be impacted by higher-order QED corrections to the box diagrams which are responsible for the leptonic-state mixing. Below we roughly estimate these effects on the determination of θ_{13} . The QED corrections to the box diagrams in the symmetric phase, where all particles are massless, do not differentiate intermediate channels. Hence, the argument for the disappearance of the mixing phenomenon, based on the unitarity of the PMNS matrix, still holds at a high energy. The corrections that differentiate various channels in the broken phase arise from the box diagrams involving intermediate neutrinos of distinct masses and a photon exchanged between two external charged leptons. These diagrams give channel-dependent contributions apparently. Since ν_1 , ν_2 and ν_3 are much lighter than ν_4 , the QED effects associated with the former are approximately the same, and differ from the one associated with ν_4 . The former contribution can be inferred from the result for the box diagram with light fermions [53], which is destructive to the leading-order one. The latter can be inferred from the heavy fermion expansion for the box diagram induced by heavy-light currents [54]; the leading piece of the expansion in the power of $1/m_4$, with the ν_4 line being shrunk to a point, represents a vertex correction. This contribution can be eliminated by choosing a renormalization scale, i.e., in the on-shell renormalization scheme. The subleading terms, suppressed by powers of $1/m_4$, are negligible. That is, the QED corrections associated with ν_4 are less important.

Relatively speaking, the considered QED effects raise the imaginary parts Γ_{i4} , $i = 1, 2$ and 3 , (Γ_{44}) by a factor $1 + \alpha(1 + 2\alpha)$ compared to the others, α being of order of the QED coupling $\alpha_e \sim 10^{-2}$. Including those correction factors into Eq. (50), we find that the right-hand side of Eq. (55) becomes $+(10\alpha/7)m_3^4/m_W^4$, where terms proportional to $m_{1,2}^2/m_{W,4}^2$ have been dropped for simplicity. This modification changes the right-hand side of Eq. (66) into $-\sqrt{10\alpha/7}m_3^2/m_W^4 \approx -5 \times 10^{-26}$ (the minus sign works better than the plus sign for increasing θ_{13}), but leaves Eq. (67) untouched. Repeating the same procedure, we solve for the ratio of the PMNS matrix elements

$$r_1 \approx -0.82 - 0.07i, \quad -1.12 + 0.07i, \quad (75)$$

which are more consistent with the data in Eqs. (71) and (72), respectively. The minimization of the deviation in Eq. (73) with $u_\mu = -0.82$, $v_\mu = -0.07$, $u_\tau = -1.12$ and $v_\tau = 0.07$ then leads to the mixing angles and CP phase

$$\theta_{23} \approx 47^\circ, \quad \theta_{13} \approx 6^\circ, \quad \delta \approx 205^\circ, \quad (76)$$

for $\theta_{12} = 34^\circ$. It is seen that θ_{13} can indeed be enlarged by the QED corrections along with slight increment of δ .

We then examine the dispersive constraints on the PMNS matrix elements in the IO scenario for the neutrino masses. Two solutions similar to Eq. (70) are acquired

$$r_1 \approx -1.032 - 0.005i, \quad -1.014 + 0.005i, \quad (77)$$

with $m_3^2 = 10^{-6} \text{ eV}^2$, and m_1^2 and m_2^2 from $\Delta m_{21}^2 = (7.50_{-0.20}^{+0.22}) \times 10^{-5} \text{ eV}^2$ and $\Delta m_{31}^2 = -(2.45_{-0.03}^{+0.02}) \times 10^{-3} \text{ eV}^2$ [51]. The results are insensitive to the variation of m_3 in this case. It is hard to associate either of them with the μe mixing. Nevertheless, it is clear that the small imaginary parts disagree with the measured ratio for the μe mixing in the IO scenario,

$$r_1 = -(1.05_{-0.18}^{+0.23}) - (0.38_{-0.05}^{+0.00})i, \quad (78)$$

corresponding to $\theta_{12} = (34.3 \pm 1.0)^\circ$, $\theta_{13} = (8.58_{-0.14}^{+0.12})^\circ$, $\theta_{23} = (49.46_{-0.97}^{+0.60})^\circ$ and $\delta = (284_{-28}^{+26})^\circ$ from [51]. In other words, the dispersive constraints refute the IO spectrum for the neutrino masses as advocated in [3].

At last, one may suspect that the existence of the massive fourth generation leptons would modify the cosmological constraint on the sum of neutrino masses $\sum m_\nu$. The neutrino masses have been assumed to be approximately degenerate in the derivation of the above constraint. The case with additional significantly massive neutrinos require a different treatment as pointed out in [55]. This subject can be addressed in a future publication. Besides, one may wonder whether the massive fourth generation neutrino could contribute to the effective neutrino masses, such as the effective Majorana mass m_{ee} , through the mixing with the light neutrinos. As explained below Eq. (59), the mixing between the light neutrinos and the fourth generation one is extremely suppressed by the factor m_i^2/m_W^2 . Therefore, the fourth generation neutrino gives $m_4 U_{e4}^2 \sim m_4 m_i^2/m_W^2 \approx 10^{-11} \text{ eV}$ to m_{ee} , where the light neutrino mass is taken as $m_i = 1 \text{ eV}$ for the estimate. This contribution is completely negligible.

VI. CONCLUSION

We have continued our efforts to constrain the parameters in the SM and beyond in dispersive analyses of physical observables. Following our previous determination for the masses of the sequential fourth generation quarks in an

extension of the SM, we have predicted the masses of the fourth generation leptons by solving the dispersion relations associated with heavy fermion decays. The approach has been elucidated in our previous works and the application to the present investigation is straightforward. The mass $m_4 \approx 170$ GeV ($m_L \approx 270$ GeV) of the fourth generation neutral (charged) lepton with little theoretical errors was extracted from the study of the $t \rightarrow de^+\nu_4$ ($L^- \rightarrow \nu_1\bar{t}d$) decay width with the input of the known top quark mass $m_t \approx 173$ GeV. The above results were then validated by means of the $L^- \rightarrow \nu_4\bar{u}d$ decay width. Although this mode suffers higher-order QCD corrections attributed to the light quark pair in the final state, the cross-check provides a solid support to our formalism and predictions. It has been inspected that the fourth generation leptons with the aforementioned masses survive the experimental bounds from Higgs boson decays into photon pairs and from the oblique parameters. Briefly speaking, the fourth generation charged lepton reduces the SM contribution to the former by 37%, and, together with the neutral lepton, enhance the oblique parameter T to 0.178. These effects are still within the current experimental uncertainties.

We discussed the dispersive constraints on the neutrino masses and the PMNS matrix elements in the presence of the fourth generation leptons. It turns out that the heavy neutrino demands the almost exact unitarity of the 3×3 PMNS matrix, and the observed ratios of the PMNS matrix elements, $U_{\mu 1}^* U_{e 1} / (U_{\mu 2}^* U_{e 2})$ and $U_{\tau 1}^* U_{e 1} / (U_{\tau 2}^* U_{e 2})$, can be better accommodated, as the known mass-squared differences Δm_{21}^2 and Δm_{32}^2 are input. This accommodation marks an improvement of our previous analysis based on three generations of neutrinos, which, in some sense, suggests the existence of the fourth generation neutrino. The constraints on the above two ratios are equivalent to those on the mixing angles and CP phase in the 3×3 PMNS matrix, giving $\theta_{12} \approx 34^\circ$, $\theta_{23} \approx 47^\circ$, $\theta_{13} \approx 5^\circ$ and $\delta \approx 200^\circ$ approximately, close to the data for the NO scenario (except θ_{13}). The above results are insensitive to the variation of the lightest neutrino mass m_1 . The consistencies of our theoretical framework in various aspects encourage the search for such heavy neutral and charged leptons at the (high-luminosity) large hadron collider or a muon collider.

Acknowledgement

We thank K.F. Chen, Y.T. Chien, Y. Chung, X.G. He, W.S. Hou, C.J. Lin, M. Spinrath and M.R. Wu for fruitful discussions. This work was supported in part by National Science and Technology Council of the Republic of China under Grant No. MOST-110-2112-M-001-026-MY3.

-
- [1] H. n. Li, Phys. Rev. D **107**, no.9, 094007 (2023).
 - [2] H. n. Li, Phys. Rev. D **108**, no.5, 054020 (2023).
 - [3] H. n. Li, [arXiv:2306.03463 [hep-ph]].
 - [4] H. n. Li, Chin. J. Phys. **92**, 1043-1054 (2024).
 - [5] H. n. Li, Phys. Rev. D **109**, no.11, 115024 (2024).
 - [6] H. n. Li, H. Umeeda, F. Xu and F. S. Yu, Phys. Lett. B **810**, 135802 (2020).
 - [7] H. n. Li, Phys. Rev. D **107**, no.5, 054023 (2023).
 - [8] A. S. Xiong, T. Wei and F. S. Yu, [arXiv:2211.13753 [hep-th]].
 - [9] S. Navas et al. (Particle Data Group), Phys. Rev. D **110**, 030001 (2024).
 - [10] B. Holdom, Phys. Rev. Lett. **57**, 2496 (1986), [Erratum-ibid. 58, 177 (1987)]; W. A. Bardeen, C. T. Hill and M. Lindner, Phys. Rev. D **41**, 1647 (1990); C. T. Hill, M. A. Luty and E. A. Paschos, Phys. Rev. D **43**, 3011 (1991); T. Elliott and S. F. King, Phys. Lett. B **283**, 371 (1992).
 - [11] Y. Mimura, W. S. Hou and H. Kohyama, JHEP **11**, 048 (2013).
 - [12] S. W. Ham, S. K. Oh and D. Son, Phys. Rev. D **71**, 015001 (2005); M. S. Carena, A. Megevand, M. Quiros and C. E. M. Wagner, Nucl. Phys. B **716**, 319 (2005); R. Fok and G. D. Kribs, Phys. Rev. D **78**, 075023 (2008) Y. Kikukawa, M. Kohda and J. Yasuda, Prog. Theor. Phys. **122**, 401-426 (2009).
 - [13] W. S. Hou, Chin. J. Phys. **47**, 134 (2009).
 - [14] P. Q. Hung and C. Xiong, Nucl. Phys. B **847**, 160-178 (2011).
 - [15] T. Enkhbat, W. S. Hou and H. Yokoya, Phys. Rev. D **84**, 094013 (2011).
 - [16] N. Chen and H. J. He, JHEP **04**, 062 (2012); O. Eberhardt, G. Herbert, H. Lacker, A. Lenz, A. Menzel, U. Nierste and M. Wiebusch, Phys. Rev. Lett. **109**, 241802 (2012); A. Djouadi and A. Lenz, Phys. Lett. B **715**, 310-314 (2012); E. Kuflik, Y. Nir and T. Volansky, Phys. Rev. Lett. **110**, no.9, 091801 (2013).
 - [17] H. J. He, N. Polonsky and S. f. Su, Phys. Rev. D **64**, 053004 (2001).
 - [18] X. Marcano, [arXiv:2405.10840 [hep-ph]].
 - [19] P. F. de Salas, D. V. Forero, C. A. Ternes, M. Tortola and J. W. F. Valle, Phys. Lett. B **782**, 633-640 (2018).
 - [20] F. Capozzi, E. Lisi, A. Marrone and A. Palazzo, Prog. Part. Nucl. Phys. **102**, 48-72 (2018).
 - [21] A. V. Manohar and W. J. Waalewijn, Phys. Rev. D **85**, 114009 (2012).
 - [22] C. W. Groetsch, J. Phys.: Conf. Ser. **73**, 012001 (2007).

- [23] D. Borwein, J. M. Borwein, R. E. Crandall, *SIAM J. Numer. Anal.* **46**, 3285–3312 (2008).
- [24] A. Ali, E. A. Kuraev and Y. M. Bystritskiy, *Eur. Phys. J. C* **67**, 377–395 (2010).
- [25] M. Jezabek and J. H. Kuhn, *Nucl. Phys. B* **320**, 20–44 (1989).
- [26] J. Yan, X. G. Wu, H. Zhou, H. T. Li and J. H. Shan, [arXiv:2404.11133 [hep-ph]].
- [27] C. H. V. Chang, D. Chang, W. F. Chang, H. n. Li and H. L. Yu, *Phys. Rev. D* **58**, 094019 (1998).
- [28] M. Bruno, M. Dalla Brida, P. Fritzsche, T. Korzec, A. Ramos, S. Schaefer, H. Simma, S. Sint and R. Sommer, *PoS LATTICE2016*, 197 (2016).
- [29] A. Deur, S. J. Brodsky and G. F. de Teramond, *Prog. Part. Nucl. Phys.* **90**, 1 (2016).
- [30] T. H. Chang, K. J. F. Gaemers and W. L. van Neerven, *Nucl. Phys. B* **202**, 407–436 (1982).
- [31] T. Alvarez, A. Leites and J. Terron, *Nucl. Phys. B* **301**, 1–14 (1988).
- [32] S. G. Gorishnii, A. L. Kataev and S. A. Larin, *Phys. Lett. B* **259**, 144–150 (1991).
- [33] L. R. Surguladze and M. A. Samuel, *Phys. Rev. Lett.* **66**, 560–563 (1991) [erratum: *Phys. Rev. Lett.* **66**, 2416 (1991)].
- [34] K. G. Chetyrkin and J. H. Kuhn, *Phys. Lett. B* **406**, 102–109 (1997).
- [35] D. Kara, *Nucl. Phys. B* **877**, 683–718 (2013).
- [36] B. C. Allanach, C. M. Harris, M. A. Parker, P. Richardson and B. R. Webber, *JHEP* **08**, 051 (2001).
- [37] L. Bellantoni, J. Erler, J. J. Heckman and E. Ramirez-Homs, *Phys. Rev. D* **86**, 034022 (2012).
- [38] O. Eberhardt, G. Herbert, H. Lacker, A. Lenz, A. Menzel, U. Nierste and M. Wiebusch, *Phys. Rev. D* **86**, 013011 (2012).
- [39] K. Ishiwata and M. B. Wise, *Phys. Rev. D* **84**, 055025 (2011).
- [40] J. Davies and F. Herren, *Phys. Rev. D* **104**, no.5, 053010 (2021).
- [41] C. Sturm, *Eur. Phys. J. C* **74**, no.8, 2978 (2014).
- [42] M. E. Peskin and T. Takeuchi, *Phys. Rev. Lett.* **65**, 964 (1990); *Phys. Rev. D* **46**, 381–409 (1992).
- [43] Y. T. Chien and H. n. Li, *Phys. Rev. D* **97**, no.5, 053006 (2018).
- [44] L. Huang, S. D. Lane, I. M. Lewis and Z. Liu, *Phys. Rev. D* **103**, no.5, 053007 (2021).
- [45] D. B. Kaplan and H. Georgi, *Phys. Lett. B* **136**, 183–186 (1984).
- [46] H. Y. Cheng, *Phys. Rev. D* **26**, 143 (1982).
- [47] A. J. Buras, W. Slominski and H. Steger, *Nucl. Phys.* **B245**, 369 (1984).
- [48] C. Y. Seng, *Mod. Phys. Lett. A* **37**, no.02, 2230002 (2022).
- [49] T. Kitahara and K. Tobioka, *Phys. Rev. D* **108**, no.11, 11 (2023).
- [50] T. Kitahara, [arXiv:2407.00122 [hep-ph]].
- [51] P. F. de Salas, D. V. Forero, S. Gariazzo, P. Martínez-Miravé, O. Mena, C. A. Ternes, M. Tórtola and J. W. F. Valle, *JHEP* **02**, 071 (2021).
- [52] F. Capozzi, E. Di Valentino, E. Lisi, A. Marrone, A. Melchiorri and A. Palazzo, *Phys. Rev. D* **104**, no.8, 083031 (2021).
- [53] E. Braaten, *Phys. Rev. D* **28**, 524 (1983).
- [54] W. Detmold *et al.* [HOPE], *Phys. Rev. D* **104**, no.7, 074511 (2021).
- [55] A. Mantz, S. W. Allen and D. Rapetti, *Mon. Not. Roy. Astron. Soc.* **406**, 1805–1814 (2010).